

Pressure Broadening of the 1.3 μm Iodine Laser Line

W. Fuß and K. Hohla

Max-Planck-Institut für Plasmaphysik, Euratom Association, Garching

(Z. Naturforsch. 31 a, 569–577 [1976]; received April 15, 1976)

The storable energy of a high-power laser is inversely proportional to its stimulated emission cross-section σ . By adding a foreign gas, the emission line is broadened and is thereby lowered. We have measured σ of the iodine laser as a function of the pressure of several gases (Ar, N₂, CO, CO₂, SF₆, CF₃Br, C₃F₇I, CF₂Cl₂, (CF₃)₂CO) by an absolute and a relative method. $1/\sigma$ is a linear function of the pressure in spite of the fact that overlapping of the hyperfine structure components varies considerably in the range investigated. For optimum energy storage, CO₂ is a good compromise between pressure broadening and chemical deactivation of the excited I-atoms. At one atmosphere of CO₂, 5 to 7 J/cm² can be stored, the hyperfine structure is largely blurred, and the amplification of pulses shorter than 100 psec should be possible.

I. Introduction

In high-power lasers energy is normally accumulated and stored in a laser amplifier until a pulse from a laser oscillator induces the amplifier to emit. A parameter of crucial importance for energy storage is the stimulated emission cross-section σ of the active medium. The inversion storable per unit cross-section is inversely proportional to σ :

$$\Delta n_{\text{st}} l = \ln V_{\text{th}} / \sigma \quad (1)$$

(n_{st} = storable inversion density, l = length of the active medium, V_{th} = threshold amplification, σ = maximum cross-section of the gain profile).

In the photochemical iodine laser σ can be varied over a large range by pressure broadening. We determined the effect of various gases (Ar, N₂, CO, CO₂, SF₆, CF₃Br, C₃F₇I, CF₂Cl₂, (CF₃)₂CO) on the σ of the iodine laser transition (1.3 μm) by combining small and large-signal gain measurements of single nanosecond pulses. In addition, some conclusions could be drawn concerning the homogeneity of the spectrum, which is of importance in the saturation behaviour of the iodine laser.

Previous workers have measured pressure broadening by He, Ar^{1,2} and CF₃I³. But in³ the hyperfine structure has not been considered; and for the measurements of¹ and² long pulses were used, in which case the influence of the recombination of ground state iodine atoms with the radicals is not well known. Further work has been done on the ratios of pressure broadening coefficients due to He and Ar^{4,5} the other noble gases, and CO₂⁵. A recent paper⁶ reports pressure broadening by CF₃I.

Reprint requests to Dr. L. Johannsen, Max-Planck-Institut für Plasmaphysik, Bibliothek, D-8046 Garching bei München.

II. The 1,3153 μm Iodine Laser Transition

a) Pressure Broadening and σ

Normally, if pressure broadening dominates over Doppler broadening and if the collisions are hard collisions^{7–9}, a line has a Lorentzian shape. Its half-width $\Delta\nu$ and its maximum cross-section σ are inversely proportional to each other:

$$\sigma = \frac{\lambda^2 A}{4\pi^2} \cdot \frac{1}{\Delta\nu} \quad (2)$$

(A = spontaneous transition rate, λ = emission wavelength). $\Delta\nu$ – and hence also $1/\sigma$ and the storable energy [see (1)] – grows linearly with the gas pressures p_i :

$$\Delta\nu = \alpha_0 + \sum_i \alpha_i p_i, \quad (3)$$

$$1/\sigma = \beta_0 + \sum_i \beta_i p_i \quad (4)$$

where α_0 and β_0 contain small contributions from Doppler broadening and from Zeeman broadening by the weak magnetic field of the flashlamps, while α_i are the broadening coefficients of various gases i with the pressure p_i . The relation between α and β is given approximately by [see Eq. (2)]

$$\alpha_i = \frac{\lambda^2 A}{4\pi^2} \beta_i. \quad (5)$$

b) The Resolved Iodine Laser Spectrum

In the case of the photochemical iodine laser the upper and lower levels of the laser transition (²P_{1/2} → ²P_{3/2}) have a hyperfine splitting (hfs)^{2,10}. According to this hfs we have six different possible lines. In Fig. 1a the various sublevels and the al-



Dieses Werk wurde im Jahr 2013 vom Verlag Zeitschrift für Naturforschung in Zusammenarbeit mit der Max-Planck-Gesellschaft zur Förderung der Wissenschaften e.V. digitalisiert und unter folgender Lizenz veröffentlicht: Creative Commons Namensnennung-Keine Bearbeitung 3.0 Deutschland Lizenz.

Zum 01.01.2015 ist eine Anpassung der Lizenzbedingungen (Entfall der Creative Commons Lizenzbedingung „Keine Bearbeitung“) beabsichtigt, um eine Nachnutzung auch im Rahmen zukünftiger wissenschaftlicher Nutzungsformen zu ermöglichen.

This work has been digitalized and published in 2013 by Verlag Zeitschrift für Naturforschung in cooperation with the Max Planck Society for the Advancement of Science under a Creative Commons Attribution-NoDerivs 3.0 Germany License.

On 01.01.2015 it is planned to change the License Conditions (the removal of the Creative Commons License condition “no derivative works”). This is to allow reuse in the area of future scientific usage.

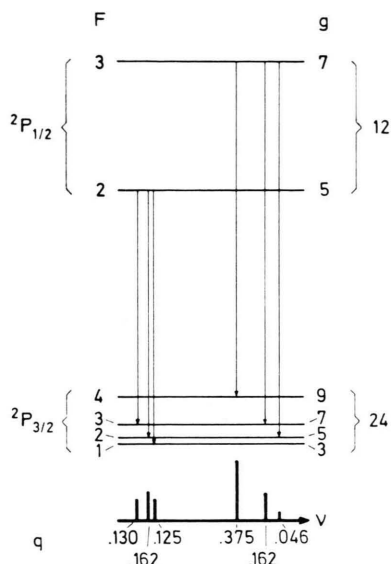


Fig. 1. Hyperfine structure of the iodine laser transition; F = quantum number of electronic plus nuclear angular momentum, g = degeneracies, q = normalized relative intensities¹¹.

lowed transitions are depicted. The F -numbers and the degeneracies g are written on the left and right sides of the levels, respectively. In the lower part of Fig. 1 the relative intensities q of the six lines are shown according to Sobel'man¹¹.

Usually, σ is defined in such a way that Δn in the product $\sigma \Delta n$ [e.g. in (1)] means the total inversion, summed over the hfs levels. This definition implies that σ is smaller by a factor $a = \Delta n_{ij} / \Delta n$ (Δn_{ij} being the inversion density between the sublevels i and j) than a cross-section based on an individual transition from sublevel i to sublevel j . (Of course, a cross-section based on an individual transition can only be defined if this transition is well resolved in the spectrum.) Similarly, A is defined such that n in the product $A \cdot n$ means the total population density in the upper levels. A has to be multiplied by a factor $a' = n_i / n$, if it is related to the upper sublevel i . Because the upper levels are initially populated in the ratio of their degeneracies, whereas the number of the ground state iodine atoms produced in the photolysis of the usual iodides is negligible^{12, 13}, a is equal to a' .

In the iodine laser, a is calculated from the ratio of the statistical weights (Fig. 1) to be 5/12 or 7/12, depending on whether the initial level is the $F=2$ or $F=3$ sublevel of the $2P_{1/2}$ state.

In any formulae where σ or A occurs without being multiplied by Δn or n [e.g. in (2) and (4)] a correction for the factor a is necessary. Thus, the half-width of the strongest iodine laser line $F=3 \rightarrow F=4$ (being equal to the half-width of the other hfs lines) is calculated from

$$\sigma_{34}/a = \frac{\lambda^2 (A/a) q_{34}}{4 \pi^2} \frac{1}{\Delta \nu} \quad (6)$$

Here σ_{34} is the cross-section at the frequency of the $F=3 \rightarrow F=4$ transition, again based on the total inversion Δn , q_{34} is the normalized intensity¹¹ (see Fig. 1) of this hfs transition. A is again the total transition probability based on the population of both the upper levels, which is calculated from¹⁴ to be equal to 7.96 s^{-1} . With $a = 7/12$ this combines to yield

$$\Delta \nu = 1.3 \cdot 10^{-9} \text{ cm}^2 \text{ Hz} \cdot (1/\sigma) \quad (6a)$$

where the index 34 on σ has been omitted, because the maximum of the $3 \rightarrow 4$ line is practically identical to the maximum of the total spectrum as long as the lines are narrow. In the same way, Eq. (5) has to be replaced provided that β_i refers to the $3 \rightarrow 4$ transition and provided that this lines is well resolved:

$$\alpha_i = 1.3 \cdot 10^{-9} \text{ cm}^2 \text{ Hz} \cdot \beta_i \quad (5a)$$

c) Broadening and Internal Relaxation

With increasing pressure broadening the lines begin to overlap. The gain profiles corresponding to the individual lines with the relative intensities of Fig. 1 must be added (Figure 2). The maximum of the resulting gain curve corresponds to a σ value (σ_{total}) which may again be used in (1). But this σ cannot be expected to fulfil a linear relation like (4) for, with increasing overlap of the lines, σ_{total} does not decrease as much with pressure as the σ of a single line. Figure 3 shows σ_{total} (called simply σ henceforth) calculated from spectra like those of Fig. 2 as a function of the width $\Delta \nu$ of a single line.

If $\Delta \nu$ is a linear function of pressure, this type of curve is also expected for $1/\sigma$ as a function of pressure. Figure 3 can be used to determine the line-width of the single lines from measured σ values, if the assumption of Lorentzian line profiles is correct.

In an intermediate broadening case like in Fig. 2b the emission can be considered as consisting of two homogeneous lines resulting from two independent upper levels with degeneracies 5 and 7 and one

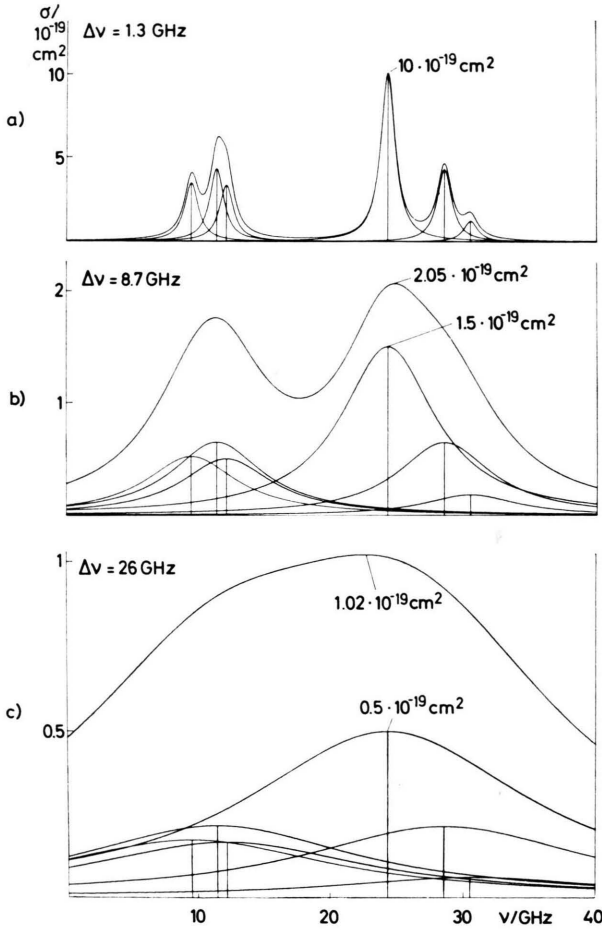


Fig. 2. Gain spectrum of the iodine laser calculated with various half-widths $\Delta\nu$ of a single line and the relative intensities from Figure 1.

lower level of statistical weight 24. A similar situation can arise for smaller line-widths, if the pulses are long enough: Yukov et al.^{16, 17} have shown that collisions efficiently induce internal relaxation among the sublevels of the ground state, whereas the $^2P_{1/2}$ sublevels relax very much more slowly. So, for a sufficiently long pulse even an only slightly broadened spectrum can appear as consisting of two homogeneous parts.

III. Measuring Method

a) Absolute Measurement of σ

The starting point for the measurement of σ is the formula for the small-signal amplification V_{ss} :

$$V_{ss} = \exp(\sigma \Delta n l). \quad (7)$$

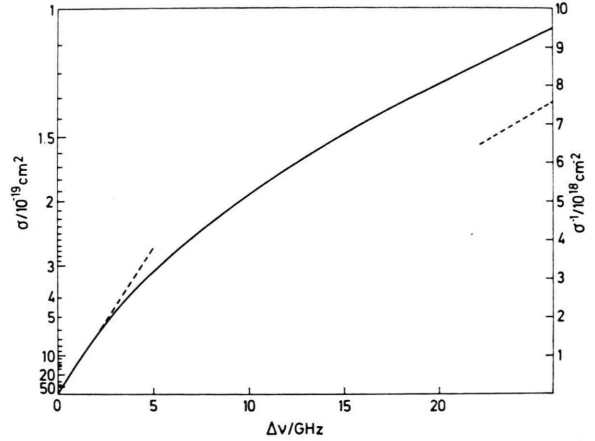


Fig. 3. $1/\sigma$ calculated as a function of the line width of a single hfs component. Owing to increasing contributions from adjacent lines, σ decreases more slowly with $\Delta\nu$ than expected for a single line (than the low pressure limit or low $\Delta\nu$ limit); ---- low and high pressure limits.

If both V_{ss} and Δn can be measured, σ can easily be calculated.

Again, σ denotes the maximum cross-section of the gain profile. Therefore, it has to be checked if the input frequency (to be amplified) is close to this maximum.

Previous workers have deduced Δn from the oscillator energy:

$$E_{osc} = (h\nu/b) (\Delta n - \Delta n_{thr}) l Q, \quad (8)$$

$$b = 1 + g_u/g_l \quad (9)$$

(Q is the geometric cross-section of the active medium, and g_u and g_l are the degeneracies of the upper and lower levels, respectively.) The threshold inversion Δn_{thr} can be eliminated by varying the threshold amplification V_{thr} , i. e. by varying the cavity losses, and extrapolating to $V_{thr} = 0$. Unfortunately, the degeneracy factor b is uncertain. On the one hand, all hfs sublevels can relax among each other within the long time involved in oscillator emission, so that the statistical weights should be taken as 12 and 24 and b should be equal to 1.5. On the other hand, some experiments indicate that the $i\text{-C}_3\text{F}_7$ radicals produced in the photolysis of $i\text{-C}_3\text{F}_7\text{I}$ rapidly recombine with ground state iodine atoms, so that b has to be set equal to 1 as in other four level lasers. So it is desirable to determine Δn and σ by short pulses.

Therefore, we measured the amplification V for small and large input energy densities e_{in} using

single one-nanosecond pulses. The saturation energy density e_s was then determined from

$$V = (e_s/e_{\text{in}}) \ln[1 + (\exp(e_{\text{in}}/e_s) - 1)V_{\text{ss}}] \quad (10)$$

by a graphical method. In the case of a homogeneous line, σ can then be calculated from

$$e_s = h \nu / b \sigma. \quad (11)$$

Two questions now arise: 1) Has the cross-section σ in (11) to be corrected in the same way as discussed in paragraph II b), i. e. has σ to be divided by a in order to convert it to a cross-section based on the inversion for an individual transition? 2) What happens to Eq. (11) if, as in the iodine laser, only part of the inversion can respond to a given input frequency, i. e. if the spectrum is not completely homogeneous?

Large-signal amplification by a single well resolved homogeneous line can obviously be treated as if the other lines did not exist, i. e. σ has in fact to be converted to a cross-section based on the corresponding individual inversion by dividing it by a . Equation (11) becomes

$$e_s = a (h \nu / b \sigma). \quad (12)$$

Depending on which of the levels emit, a is equal to the fractional population of either the $F=3$ level ($a=7/12$) or the $F=2$ level ($a=5/12$). For line widths similar to those of Fig. 2 b the spectrum consists of two homogeneous parts. Equation (12) is again valid, $a=7/12$, if the emission is in the high-frequency part of the spectrum, and $a=5/12$ for the low-frequency part. If the line widths are much larger than the line distances, the whole spectrum is homogeneous; in this case (11) has to be used or, alternatively, one has to set $a=1$ in (12).

So, a can be looked at as a parameter characterizing homogeneity. It is just the fraction of the inversion which can respond to the input frequency. But it has to be remembered that in intermediate broadening cases, where the spectrum cannot be divided into homogeneous parts, Eq. (10) cannot be applied and therefore e_s and a are not defined.

The degeneracy factor b in Eq. (12), which is calculated from (9), again depends on the input frequency, the degree of overlap, and the ratios of the relaxation times to the pulse duration. g_u and g_l in Eq. (9) are the effective statistical weights of the upper and lower levels respectively, i. e. the sum of the degeneracies of the levels involved in the emission.

b) Relative Measurements of σ

Once a σ value at low pressure p_0 has been settled, further values at higher foreign gas pressures p_M can be determined simply by measuring the small-signal amplification V_{ss} . From (7) it follows that

$$\sigma(p_M) = \frac{\lg V_{\text{ss}}(p_M)}{\lg V_{\text{ss}}(p_0)} \sigma(p_0). \quad (13)$$

This type of measurement can also be done at pressures (p_M) where a and b are not well defined and where (10) cannot be applied. Equation (13) contains the assumption that the inversion density Δn produced by photolysis does not depend on foreign gas pressure. We checked this condition by measuring the oscillator energy at low and high p_M .

IV. Experiments

a) Set-up for Absolute σ Measurements

The absolute measurements of σ (large and small-signal gains) were made with the set-up in Figure 4. The oscillator and pulsecutting system are described in ¹⁸. The oscillator is operated in TEM₀₀ mode and is acousto-optically mode-locked. Filled with 100 torr $i\text{-C}_3\text{F}_7\text{I}$, it emits a pulse train of 1 ns pulses. The cutting system (Glan prism, Pockels cell, Glan prism) extracts from this train a single pulse of about 0.5 mJ energy. By means of Fabry-Perot measurements of the frequency-doubled pulses, we found ¹⁹ that these pulses, cut out of the beginning of the train, only contain the frequency corresponding to the high-frequency part of the spectrum. This is an indication ¹⁹ that Zeeman splitting of the lines by the magnetic field of the flash lamps can be disregarded in our configuration of pairs of parallel flashlamps. It was also disregarded in the amplifiers.

The preamplifier was only used for the one high-pressure measurement, at 50 torr $\text{C}_3\text{F}_7\text{I} + 700$ torr CO_2 , in order to reach the saturation energy at this pressure. When the preamplifier was flashed with 1 kJ of electrical energy, with a filling pressure of 200 torr of $\text{C}_3\text{F}_7\text{I}$, the pulse at the entrance of the main amplifier had an energy of 30 to 40 mJ. The beam diameter at this point was around 4 mm.

This beam passes through the centre of the main amplifier tube. Its inner diameter was 25 mm; 80 cm of its length was flashed with two pairs of parallel flashlamps, supplied with an electrical energy of 600 J in the low-pressure measurements, and 3 kJ otherwise. At the exit of the amplifier, a diaphragm cut out the central 5 mm² of the beam in order to fulfil the requirement of equal energy den-

sity over the beam cross-section for the large-signal gain measurements.

Portions of the input and output pulses arrived with a time delay at the same detector, a Valvo XA 1003 vacuum photodiode. The time resolution of the set-up (diode, cable, and Tektronix 7704 oscilloscope) was just somewhat poorer than the pulse length (~ 1 nsec); thus it was the energy amplification that was measured. For small-signal amplification measurements, the preamplifier was not operated, and the input pulse was attenuated by a factor of 500 to 5000. The input energy density was calculated from the output energy, the beam cross-section after the diaphragm, and the amplification. The output energy was measured with a Quantronix 504 calorimeter with head 500, which was compared with a Cilas CG 64 calorimeter. Since both instruments agreed within 5 per cent, they were taken to be sufficiently exact.

b) Set-up for Relative σ Measurements

Most of the relative measurements of σ (small-signal gain ratios) were done with the simpler set-up of Figure 5. The flashlamps of the oscillator were fed with 2 kJ of electrical energy lasting about 2.5 ms. With a filling of 2 torr $\text{C}_3\text{F}_7\text{I}$ + 20 torr SF_6 , the oscillator emission was about 2 ms long and fairly smooth. At this low pressure, the oscillator line widths can be expected to be not much more than the Doppler width. Since the pressure used in the amplifier were higher (20 torr $\text{C}_3\text{F}_7\text{I}$ + foreign gas) it is the σ value of the amplifier line centre which was measured. The spectral output of the oscillator was unknown. But relative measurements done with the set-up in Fig. 4 for Ar and CO_2 it was shown that the results agreed within 5 per cent. The amplifier was pumped by a pair of flashlamps supplied with 900 J of electrical energy for about 3 μs . For every gas a series of measurements was done: 20 torr of pure $\text{C}_3\text{F}_7\text{I}$ resulted in an amplification of about 1000; then mixtures of 20 torr of $\text{C}_3\text{F}_7\text{I}$ with increasing contents of foreign gas (almost to one atmosphere) were taken until the amplification was of the order of 2. This corresponds to a lowering of σ by a factor of 10.

Deactivation of the iodine atoms by the foreign gas reduces the amplification, too. If only the small-signal amplification is measured, as in the relative measurements, care has to be taken to distinguish this effect from pressure broadening. The long oscillator signal allowed deactivation constants to be determined separately, simply by looking at the decay of the amplification. At higher pressures, these measurements are perturbed by sound waves deflecting the beam. The first one arrives about

50 μs after the flash at the centre of the amplifier tube (24 mm diameter). Their effect is essentially neutralized by the lens of short focal length in front of the photomultiplier tube (RCA 7102).

V. Results and Discussion

a) The Right Choice of a and b

Our absolute σ values, obtained from the saturation energies, are based on the assumption $a = 7/12$, $b = 1.78$ at low pressures and $a = 1$, $b = 1.5$ at 50 torr $\text{C}_3\text{F}_7\text{I}$ + 700 torr CO_2 . This choice of parameters can be justified in two ways:

1) At low pressure (up to about 250 torr of argon), the relaxation time of the lower levels can be estimated to be greater than the measuring time of 1 ns^{16, 17}. Furthermore, down to $\sigma = 7 \cdot 10^{-19} \text{ cm}^2$, the overlapping of the $3 \rightarrow 4$ line with adjacent lines is calculated to be negligible. Thus, only the levels $^2\text{P}_{1/2}$ ($F = 3$) and $^2\text{P}_{3/2}$ ($F = 4$) are involved in the amplification of our single-frequency input pulse. In the high-pressure measurement, however, overlapping of the hfs lines was already substantial (intermediate between Fig. 2 b and 2 c) so that at the high input energy density all levels could respond to the input frequency. But the limit $a = 1$ was probably not quite attained.

2) If different a and b parameters are chosen, different absolute σ values are obtained. The relative σ values based on them change in the same ratio, according to (13):

$$\begin{aligned} \sigma_{\text{rel}} &= \frac{\lg V_{\text{ss}}(p_M)}{\lg V_{\text{ss}}(p_0)} \sigma_{\text{abs}}(p_0) \\ &= \frac{\lg V_{\text{ss}}(p_M)}{\lg V_{\text{ss}}(p_0)} \frac{a}{b} \frac{h\nu}{e_s(p_0)}, \end{aligned} \quad (13)$$

where a/b also depends on the pressure p_0 . When the data for V_{ss} and e_s at either low or high pressure p_0 of CO_2 were inserted into (13), varying of a/b as a parameter resulted in the set of straight lines of Figure 6.

The three pairs of a and b values given in Fig. 6 correspond to the three cases

- $a = 7/12$, $b = 1 + 7/9$, $a/b = 0.33$: no relaxation, no spectral overlap (Fig. 2 a),
- $a = 7/12$, $b = 1 + 7/24$, $a/b = 0.45$: fast relaxation among the lower levels only or spectral overlapping of the lines with a common upper level, but vanishing overlapping of lines with different upper levels (Fig. 2 b),

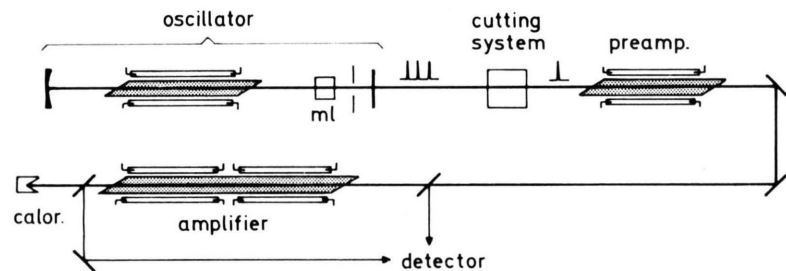


Fig. 4. Set-up for determination of σ by ns pulses. ml acoustooptical mode-locker.

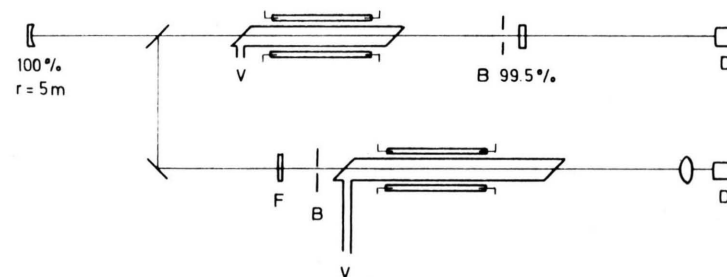


Fig. 5. Set-up for determination of σ and of deactivation rates by ms pulses. *B* diaphragm, *F* filter, *D* photomultiplier, *V* vacuum line.

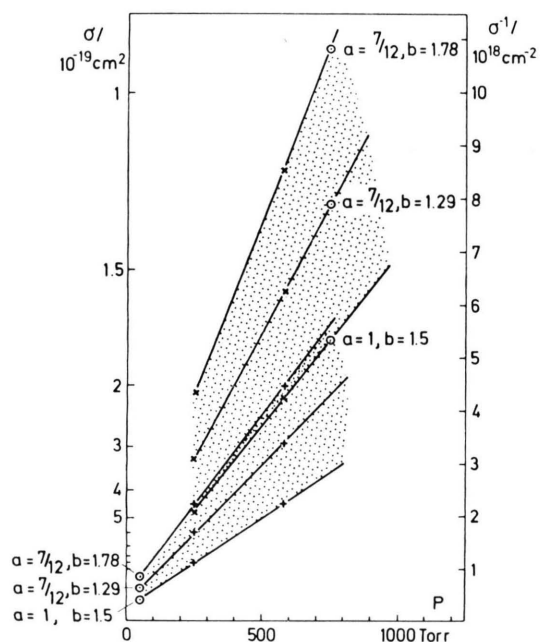


Fig. 6. $1/\sigma$ as a function of CO_2 pressure, assuming different a and b parameters. \odot according to absolute measurements, assuming different a/b values, $+$ according to relative measurements and based on low pressure \odot , \times according to relative measurements and based on high pressure \odot .

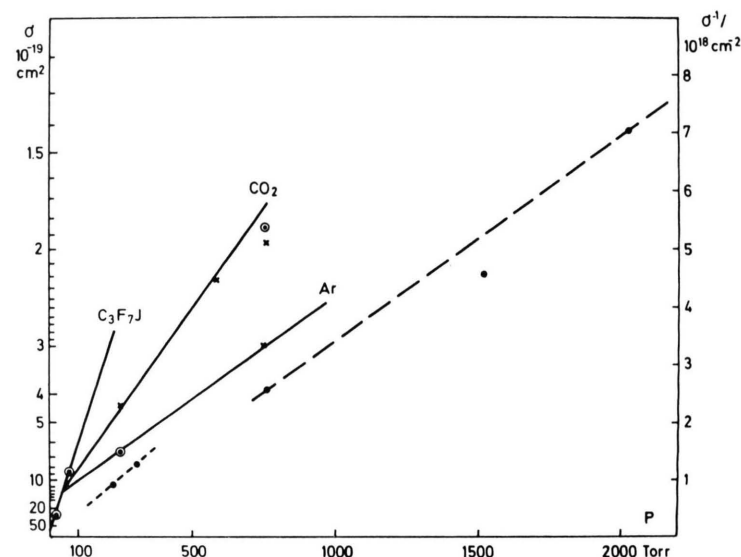


Fig. 7. $1/\sigma$ as a function of pressure of 1. pure $\text{C}_3\text{F}_7\text{I}$, 2. $\text{Ar} + 50$ torr $\text{C}_3\text{F}_7\text{I}$, 3. $\text{CO}_2 + 50$ torr $\text{C}_3\text{F}_7\text{I}$. \odot absolute measurement; \times relative measurement, both done with ns pulses. For comparison the absolute measurements of Aldridge¹ (—) and Zujev et al.² (---), both for Ar at a very small iodine pressure, have been included.

- c) $a=1$, $b=1+12/24$, $a/b=0.67$: fast relaxation among the lower levels and among the upper levels or complete blurring of the hyperfine structure (not quite attained in Figure 2 c).

Figure 6 shows that only one set of a and b parameters exists that makes the relative σ values consistent (i. e. brings + and \times crosses to coincidence) irrespective of whether they are based on the low or high-pressure absolute σ . This set corresponds to case a) at low pressure and case c) at high pressure.

b) σ as a Function of Pressure

Figure 7 shows the data obtained from the nanosecond pulse set-up. In this figure, σ is plotted versus the pressure p_M of the broadening gas $\text{C}_3\text{F}_7\text{I}$, CO_2 and Ar. The slopes of the straight lines are the β_M coefficients defined by Equation (4). The accuracy of the absolute values of σ is mainly limited by the accuracy in the measurement of the energy density which we estimate to be ± 20 per cent. The measurements were reproducible within about ± 5 per cent. Included in the figure are literature data^{1,2} for argon at low iodide pressure, which have been measured using long pulses. The agreement of the slopes is remarkable.

The quoted authors^{1,2} took an a/b value of 0.67 because for longer emission times case c) is expected to be valid. The agreement of their σ values with our ns pulse measurements confirms their assumption. However, in our measurements with long pulses we found quite another value of a/b , namely $a/b=1$. This difference may be due to the much higher photolysis density we achieved in our apparatus (10 torr of iodine atoms, typically; flash duration $\sim 5 \mu\text{s}$). Our explanation is that in our case essentially all excited iodine atoms can emit because of the fast recombination of ground state iodine atoms with the C_3F_7 radicals²⁰. This infers that $a/b=1$.

While behaviour like that in Fig. 3 was expected for $1/\sigma$ as a function of pressure, we have connected our data points in Fig. 7 by straight lines, because over our limited range of these two types of functions could not clearly be distinguished. Therefore, our data can be extrapolated to higher pressures only with due caution. On the other hand, the data of Aldridge in Fig. 7 indicate that a linear relation between $1/\sigma$ and pressure holds up to 2000 torr Argon. If the proportionality (6) of $1/\sigma$ and the half-width $\Delta\nu$ of a single line is assumed to hold at

least approximately, a linear relation between $1/\sigma$ and pressure implies that $\Delta\nu$ temporarily grows faster than linearly with foreign gas pressure. Such behaviour was observed⁹ at much higher pressures when the collision partners pass a potential minimum during the collision. But then deviations from the Lorentzian line profile are also observed⁹.

c) The Extraction Efficiency a/b

The parameter a reflects the degree of homogeneity of the gain spectrum and a/b is directly equal to the maximum extraction efficiency. The result $a/b=0.67$ at high pressure therefore demonstrates that already at a pressure resulting in $\sigma=1.8 \cdot 10^{-19} \text{ cm}^2$, which is close to the optimum of σ for energy storage (see Sect. VI), the stored inversion can be extracted up to 67 per cent by a single frequency pulse. This efficiency is twice the low pressure value. The result $a=1$ at high pressure implies that the gain spectrum is homogeneous; this means that saturation at one frequency reduces the gain homogeneously at all frequencies.

d) Broadening and Deactivation by Various Gases

Broadening by the other gases was only followed down to $\sigma=3$ to $4 \cdot 10^{-19} \text{ cm}^2$. In this range again, a linear dependence of $1/\sigma$ on the gas pressure p_M was found. The "broadening coefficients" β_M defined by Eq. (4) are listed in the table for all gases investigated by us and by previous workers. The relative measurements of Aldridge⁴ and Padrick and Palmer⁵ are based on Hohla's value for CF_3I ³.

Whereas the agreement of the β_{Ar} values of^{1,2,4} with ours is quite good, we cannot explain the deviations from the experimental results of⁵. At low pressure, the broadening coefficients α_M defined by Eq. (3) can be calculated from β_M and Equation (5 a). The result for argon, for example, is 4.6 MHz/torr; this compares favourably with a value of 4.3 MHz/torr, which was theoretically estimated by assuming a Lennard-Jones potential for the collision⁵. The table shows that the β_M coefficients vary considerably with the nature of the gas. However, the most effective gases also strongly quench the excited iodine atoms. Deactivation constants are also given in the table. These were used to calculate the foreign gas pressure P_{10} , which deactivates 10 per cent of the inversion in $10 \mu\text{s}$. (One cannot

M	$\beta_M/10^{15}$ $\text{cm}^{-2} \text{Torr}^{-1}$	$k_M/10^{-16}$ $\text{cm}^3 \text{s}^{-1}$	Ref.	P_{10}/Torr	$\sigma/10^{-19} \text{cm}^2$ at P_{10}	at 700 Torr
Ar	3.6	≤ 0.02	15	≥ 170000		4.0
N ₂	5.1	2	15	1700	1.15	2.8
CO	6.3	12	15	280	5.7	
CO ₂	7.0 ^d	1.5	15	2200	0.65	2.0
	7.3 ^e	4.6	b	700		1.95
SF ₆	5.0	0.24	15	14000		2.9
CF ₂ Cl ₂	11.3	25	b	135	6.6	
i-C ₃ F ₇ I	15.5	8.0	6 ^b	420	1.5	
CF ₃ Br	5.4	— ^c		(600) ^c	3.1	
(CF ₃) ₂ CO	14.4	— ^c		(350) ^c	2.0	
Previous work:			Ref. a			
He	3.1	4				
	3.8	5				
Ne	4.6	5				
Ar	3.8	4				
	3.6	1				
	4.1	2				
	5.4	5				
Kr	4.7	5				
Xe	3.2	5				
N ₂	6.6	5				
CO ₂	7.9	5				
CF ₃ I	8.7	3				
	7.5	6				

Table 1. Pressure broadening coefficients β_M , deactivation rate constants k_M , permissible pressures P_{10} , and attainable values for several gases M.

^a Deduction of data from ³, ⁴ and ⁵ has been done assuming that in ³ $a = 7/12$ instead of 1 and $b = 1.78$ instead of 1.5;

^b this work;

^c in combination with CF₃I nonexponential decay; P_{10} only in combination with CF₃I;

^d absolute measurement;

^e relative measurement.

use much longer pumping times because of pressure waves penetrating the medium from the wall with approximately sound velocity.)

VI. Conclusion

Present-day optical technology limits the maximum load of optical components such as mirrors and windows to about 5 GW/cm². If the total energy of a laser amplifier is to be extracted in a one-nanosecond pulse, there is no use in storing much more than 5 J/cm² in the amplifier. Assuming a threshold amplification 1000, which is easily attained experimentally, a stored energy density of 5 J/cm² would be possible in the iodine laser according to Eq. (1) if $\sigma \approx 2 \cdot 10^{-19} \text{cm}^2$. Obviously, this desired σ value can be attained with several

gases, especially with Ar, N₂, and CO₂, in the case of CO₂ even at atmospheric pressure. Unfortunately, our measurement of the deactivation constant indicates that the pressure of CO₂ should not exceed 700 torrs. If lower σ values are desired, Ar should be preferred.

At a σ value of $2 \cdot 10^{-19} \text{cm}^2$ the hyperfine structure is already extensively blurred (Figure 2). The total half-width is then more than 35 GHz, which should allow pulses shorter than 100 ps to be produced and amplified.

We should like to thank G. Baiker for his valuable technical assistance and Dr. R. Volk for measuring the spectral composition of our laser pulses. This work was performed under the terms of the agreement on association between Max-Planck-Institut für Plasmaphysik and Euratom.

¹ F. T. Aldridge, IEEE QE-11, 215 [1975].

² V. S. Zujev, V. A. Katulin, V. Ju. Nosač, and O. Ju. Nosač, ŽÉTF 62, 1673 [1972].

³ K. Hohla, Dissertation, Universität München 1971; IPP-Report IV/33, 1971.

⁴ F. T. Aldridge, Appl. Phys. Lett. 22, 180 [1973].

⁵ T. D. Padrick and R. E. Palmer, J. Chem. Phys. 62, (8) 3350 [1975].

⁶ V. Yu. Zalesskii and S. S. Polikarpov, Sov. J. Quant. Electron. 5, (7) 826 [1975]; their broadening coefficient has to be divided by their factor C_1 and multiplied by the speed of light to transform it to our units.

⁷ A. E. Siegman, An Introduction to Lasers and Masers, McGraw Hill, New York 1971.

⁸ R. G. Breene, The Shift and Shape of Spectral Lines, Pergamon, Oxford 1961.

- ⁹ W. R. Hindmarsh and J. M. Farr, Collision Broadening of Spectral Lines by Neutral Atoms, in J. H. Sanders, S. Stenholm (ed.), Progress in Quantum Electronics, Vol. 2 Part 3, Pergamon, Oxford 1972.
- ¹⁰ W. C. Hwang and J. V. V. Kasper, Chem. Phys. Lett. **13**, 511 [1972].
- ¹¹ Identical with $Q(IJF; IJ'F')$ of § 31 and 32 of I.I. Sobel'man, Introduction to the Theory of Atomic Spectra, Pergamon, Oxford 1972.
- ¹² S. J. Riley and K. R. Wilson, J. Chem. Soc. Faraday Disc. **53**, 133 [1972].
- ¹³ T. Donohue and J. R. Wiesenfeld, Chem. Phys. Lett. **33**, 176 [1975].
- ¹⁴ R. H. Garstang, J. Res. Nat. Bur. Stand. **A 68**, 61 [1964]; G. H. Shortley, Phys. Rev. **57**, 225 [1940]; the calculated spontaneous transition rate $A_{\text{total}} = 7.96 \text{ sec}^{-1}$ is to be preferred to the experimental ones ^{14a} which are all smaller; since the calculation of the magnetic dipole part of the transition rate does not involve any approximation, the actual value should be greater than $A_{\text{magnetic}} = 7.904 \text{ sec}^{-1}$.
- ^{14a} A survey of experimental values can be found in ¹⁵; a further value in ².
- ¹⁵ R. J. Donovan and D. Husain, Chem. Soc. London Ann. Reports **A 68**, 148 [1971].
- ¹⁶ E. A. Yukov, Sov. J. Quant. El. **3**, 117 [1973].
- ¹⁷ V. A. Alekseev, T. L. Andreeva, V. N. Volkov, and E. A. Yukov, Sov. Phys. JETP **36**, 238 [1973].
- ¹⁸ K. Hohla, IPP-Report IV/79 [1975].
- ¹⁹ R. Volk, to be published.
- ²⁰ S. V. Kuznetsova and A. I. Maslov, Sov. J. Quant. Electron. **3**, 468 [1974].
- ²¹ V. Yu. Zalesskii and T. I. Krupenikova, Optics and Spectroscopy **30**, 439 [1973].